Plasmonics (2013) 8:869–875
DOI 10.1007/s11468-013-9484-3

Enhanced Single-Molecule Spontaneous Emission in an Optimized Nanoantenna with Plasmonic Gratings

Hongming Shen · Guowei Lu · Tianyue Zhang · Jie Liu · Qihuang Gong

Received: 19 July 2012 / Accepted: 6 January 2013 / Published online: 16 January 2013
© Springer Science+Business Media New York 2013

Abstract In this study, we theoretically investigated the single-molecule fluorescence enhancement in a slit–groove structure. The excitation field enhancement, modified quantum efficiency, collection efficiency, and position dependence of a single-molecule spontaneous emission coupled to a plasmonic antenna are explored together. Simulation results revealed that the metal gratings play a crucial role in strengthening the local electromagnetic field enhancement in the excitation process and beaming the radiation light into a tiny angular volume in the emission process, whereas the total radiative decay rate and quantum efficiency are mainly determined by the slit cavity. Our findings provide an intuitive guideline to further optimize the plasmonic antenna for single-molecule detection and the results make a promising route to the development of photonic devices for the manipulation of single-molecule spontaneous emission.

Keywords Nanoantennas · Single molecule · Fluorescence enhancement · Emission directivity · Plasmonic gratings

Introduction

Optical nanoantennas, based on metallic structures, provide an efficient way to detect the weak fluorescence signal emitted by a single molecule. Up to now, various types of metallic nanostructures [1–8] have already been reported to tailor the excitation and emission processes, yet few of them can simultaneously realize bright emission intensity and narrow directivity. In recent years, optical nanoantennas with plasmonic gratings have received considerable interest for their outstanding abilities to enhance the fluorescence intensity and narrow the emission directivity [9]. This leads to a wide range of fluorescence-based applications in molecule sensing and spectroscopy [10], semiconductor lasers [11], photoelectric devices [12, 13], and quantum communication.

A series of experimental and theoretical studies have been carried out to explore the slit (hole)–groove antennas' characteristics, such as the physical mechanisms of extraordinary transmission phenomena and analytical theories for beaming light [9, 14–16]. All these properties are of practical significance to improve the effectiveness of single-molecule detection. A few groups have already reported fluorescence emission enhancement from molecules or quantum emitters located within the plasmonic nanoapertures or nanoslits surrounded by certain numbers of metal gratings. Aouani et al. have recently presented that remarkable fluorescence enhancement factor up to 120-fold with narrow radiation pattern in a cone of ±15° was obtained with an optimized bull's eyes structure [17]. The dependence of fluorescence enhancement on the number of corrugations N was also explored in ref. [18], which indicated a kind of enhancement saturation effect when increasing the number of corrugations. The excitation and emission gains in the total fluorescence process are quantified using the single-molecule fluorescence correlation spectroscopy method [17–20]. Moreover, there has been growing interest around directional control on the emission. The slit (hole)-to-first-groove distance (g) is crucial to flexibly tune the fluorescence directivity [21–23]. However, a full cognition on how the slit–groove antenna influences the single-molecule fluorescence behavior is still lacking. Many efforts are needed to further complete the physical picture of the interaction between a single molecule and a slit–groove antenna.

Electronic supplementary material The online version of this article (doi:10.1007/s11468-013-9484-3) contains supplementary material, which is available to authorized users.

H. Shen · G. Lu (✉) · T. Zhang · J. Liu · Q. Gong (✉)
State Key Laboratory for Mesoscopic Physics,
Department of Physics, Peking University, Beijing 100871, China
e-mail: guowei.lu@pku.edu.cn
e-mail: qhgong@pku.edu.cn

Here, we focus on a configuration consisting of a single subwavelength slit flanked by periodic grooves milled in a thick gold film. We theoretically investigate the single-molecule spontaneous emission with the slit–groove structure, taking into account the excitation field enhancement, modified quantum efficiency, collection efficiency, and position dependence. Firstly, we optimize the far-field radiation patterns of the antenna, which are obtained by near-to-far-field (NTFF) transformation analysis. Then, field enhancement, quantum efficiency, and radiation pattern are calculated to analyze the fluorescence enhancement by employing a two-dimensional (2D) finite-difference time-domain (FDTD) method. The position dependence of a single oriented dipole in the slit cavity is also explored for experimental requirements. Our work explicitly clarifies how the different parameters of the slit–groove structures affect the fluorescence process, and our results are in satisfactory agreement with the experimental phenomena as reported previously.

Simulation Model

Figure 1 shows a schematic of an antenna structure investigated in our simulations, consisting of a nanoscale slit surrounded by six grooves symmetrically on both sides. Gold was chosen as the antenna material for its better performance in the visible range than aluminum [24]. The experimental dielectric constant was obtained from ref. [25] and was molded by employing a Drude–Lorentz dispersion relation. The whole slit is filled with water (with dielectric constant ε=1.77), as well as the upper half space, whereas the substrate medium is considered to be silica (with dielectric constant ε=2.25). As depicted in Fig. 1, the excitation is normally incident from upside of the metal with linearly polarized plane wave at 633 nm. Additionally, an oriented electrical dipole emitter is placed in the center of the slit with emission wavelength of 670 nm. In experimental terms, it corresponds to a widely used fluorescent molecule called cyanine 5 (Cy5) dye with maximum absorption/emission peaks around 650/670 nm. It is noted that our simulation results are performed by using a 2D numerical FDTD method, which has been extensively tested and applied in the calculation of plasmonic metallic nanostructures [21, 23, 26, 27]. In all cases, we adopted perfectly matched layer absorption boundary conditions and the mesh pitch is set to be 1 nm (unless otherwise stated). For the purpose of discussion, we have to specify here all the antenna's geometric parameters: number of grooves N, groove periodicity G, slit-to-first-groove distance g, groove depth d, groove width a, slit thickness H, and width W (as indicated in Fig. 1).

Results and Discussions

To seek an optimized antenna structure for large enhancement factor and narrow directivity, optimization of bull's eyes structures for transmission enhancement, which has been comprehensively explored in [28], could be useful. But, as a directive antenna, we were more concerned about the angular distribution of single-molecule fluorescent emission. Hence, we performed NTFF transformation [21, 29, 30], which is demonstrated explicitly in the Supporting Information, to explore how the geometric features influence the radiation patterns. For convenience, we set the slit-to-first-groove distance g equal to groove periodicity G and number of grooves N was fixed to 6, and the parameters are close to the enhancement saturation condition [18, 28]. We summarize the geometric parameters (see Fig. 7 of the Supporting Information): N, G (g), and d are crucial to the momentum matching for field enhancement and beaming light, whereas H and W mainly contribute to the quantum efficiency enhancement. Interestingly, we also find that the groove width a close to half the periodicity G is ideal, which is in agreement with the previous study [28]. After many attempts, the optimized geometric parameters for our simulation are obtained as follows: G=g=390 nm, H=260 nm, W=80 nm, a=G/2=195 nm, d=30 nm, and N=6.

As we know, the fluorescence process can be considered approximately as two processes in theory: the excitation process and the emission process. Both the fluorescence enhancement factor and emission directivity are crucial characteristics of nanoantennas for enhanced molecular fluorescence detection. Here, we are interested in how the slit–groove antenna affects the fluorescence behaviors of a single molecule. Undoubtedly, the metal gratings play an important role in the fluorescence enhancement process. For comparison, we simulate two cases: a single slit without gratings and a single slit surrounded by finite numbers of gratings. We placed an oriented dipole in the center of a slit, which is referred to as an emitter of two-level system with ground state $|g>$ and excited state $|e>$. Thus, the fluorescence enhancement can be written as [17, 26, 31]:

$$\frac{S_f}{S_{f0}} = \frac{I}{I_0} \cdot \frac{k}{k_0} \cdot \frac{\eta}{\eta_0} \tag{1}$$

where S_f and S_{f0} are fluorescence signals detected from an emitter with and without plasmonic antennas, respectively; the factor $I/I_0 = |E|^2 \Big/ |E_0|^2$ represents a local field enhancement to quantify the excitation gain, whereas the factors k/k_0 and η/η_0 are the modifications of collection efficiency and quantum efficiency to quantify the emission gain. Based on the Poynting's theory for spontaneous emission enhancement [27], we estimated the excitation and emission gains contributing to the total fluorescence

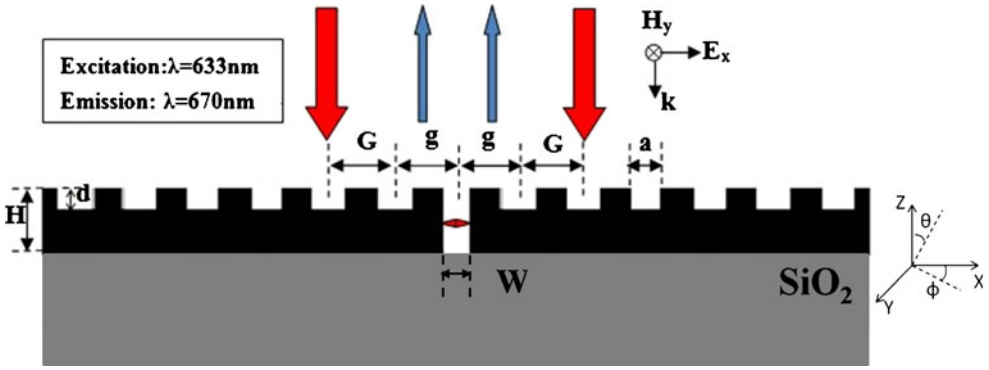

Fig. 1 Schematic of a symmetrical slit–groove structure milled in a gold film. An electrical dipole emitter, oriented in the *x*-direction, is placed in the center of the slit. The structure is illuminated with p-polarized planar continuous light at normal incidence. Optimized geometric parameters are obtained to produce a collimated beam normal to the metal surface ($G=g=390$ nm, $H=260$ nm, $W=80$ nm, $a=G/2=195$ nm, $d=30$ nm, and $N=6$)

enhancement and explored different roles of the metal gratings acting in the excitation and emission processes.

To simulate the excitation process, we calculated the local electromagnetic field distributions in the vicinity of a slit, as shown in Fig. 2. The p-polarized illumination light at a wavelength of 633 nm is incident from above. Figure 2a, b is the time-averaged field distributions for a single slit without gratings and with symmetric gratings, respectively. As we can see, large local field enhancement is obtained by introducing the metal gratings. Specially, the field intensities at the slit center and four corners are much higher, which is ascribed to the slit cavity modes determined by parameters *H* and *W*. The corresponding field enhancements with respect to the free space along $Z=0$ and $X=0$ are also shown in Fig. 2c, d. The metal gratings play a crucial role in the excitation field enhancement process. As we know, light cannot directly excite surface plasmon polaritons (SPPs) due to momentum mismatch. One of the main contributions of the side grooves is to provide necessary momentum matching to induce SPP modes [23]. Therefore, light can couple to the metal gratings (acting as an input surface) effectively when incident from above the metal/water interface. The induced SPPs then transfer along the metal surface and converge in the slit. This would also result in a remarkably sharp peak in the transmission or absorption spectrum, as presented in Fig. 8 of the Supporting Information. Moreover, two coupling mechanisms have been proposed previously [14, 32]: slit waveguide modes and induced SPP

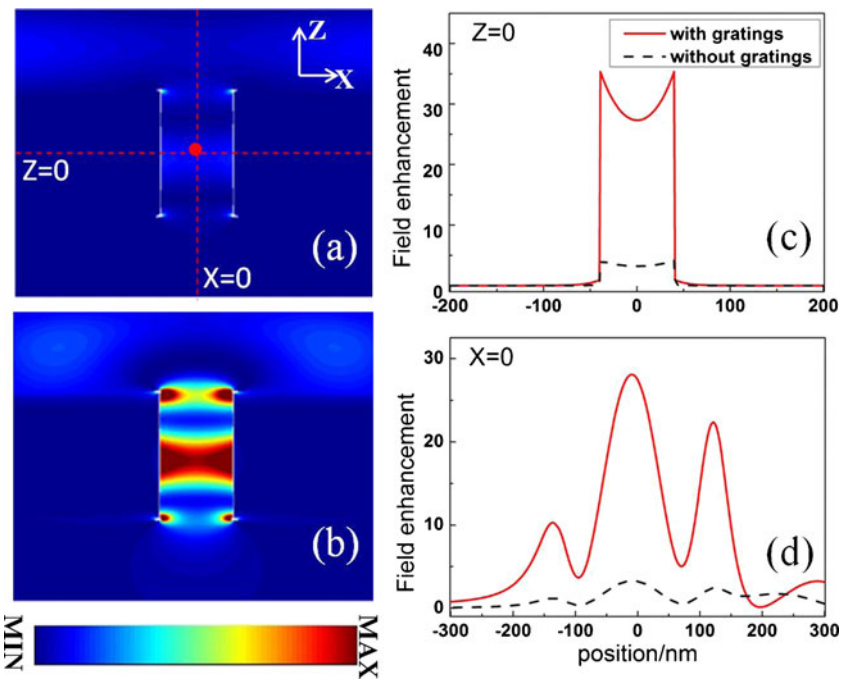

Fig. 2 Field distributions and field enhancements in the slit nanostructures. Time-averaged field distributions for **a** a single slit without gratings and **b** a slit with symmetric gratings. For comparison, **a** and **b** share the same color bar. Corresponding field enhancements relative to the free space along the **c** $Z=0$ and **d** $X=0$ in the *x*–*z* plane

resonances. We find that much larger field enhancement factor can be achieved when the resonance peaks of the SPPs and slit waveguide are consistent with each other. We also observed that the resonance peak of the absorption spectrum is primarily determined by the metal gratings. By tuning the parameters (*G*, *d*, *H*, and *W*), it is possible to obtain the maximum field enhancement factor. However, the full width at half maximum of the absorption spectrum is only around 50 nm, as shown in Fig. 8 of the Supporting Information. This indicates that it is difficult to obtain optimal field enhancement factor and narrow directivity simultaneously because of large stocks shift of photoluminescence, which we detail hereafter. Hence, there should be a tradeoff between excitation and emission processes. We set the absorption peak of the slit–grooves at a wavelength of ~650 nm to obtain relatively satisfactory field enhancement and emission directivity.

To characterize the emission process, at first, Fig. 3a presents typical far-field radiation patterns for antennas with and without gratings. From the antenna theory, directivity is a well-known physical quantity to measure the ability of beaming light, which is defined as $D(\theta) = \pi P(\theta) / \int P(\theta) \mathrm{d}\theta$ [17, 21]. We performed the NTFF transformation to calculate the angular radiation power density $P(\theta)$ and normalized it by integrating over all emission directions. As we can see in Fig. 3a, dipole emission from a single slit without gratings diffracts over a wide range of angle, which leads to a low collection efficiency and carries no information for the directions. Yet for the case of antenna with gratings, we observed a collimated beam normal to the metal surface with a half width at half maximum of ±10°. The beaming light is mainly due to a constructive interference between two components: direct transmission component from the slit and induced SPPs from the grooves [15, 22, 32].

In the emission process, the grooves (acting as an output surface) mainly contribute to the amplitude and phase lag of SPPs. Hence, we can control the emission direction by designing the grooves structure, which makes it favorable for applications in filters or sorters for fluorescence detection [23]. To give an intuitive view, we also provide normalized angular radiation patterns in the polar diagram of a dipole emission from three cases: the slit–groove structure, water/SiO_2 interface, and homogeneous medium of air, as shown in Fig. 3b. It is noted that dipole emission to the upper half space is 50 % when placed in air (blue dashed line). Yet the radiated power is more likely to emit in the denser medium when placed close to a dielectric interface (black line), which is in agreement with the recent report about a planar dielectric antenna to realize near-unity collection efficiency [33]. Interestingly, we find that the total power emission to the upper half space is slightly larger than the lower half space (about 1.4-fold) with the introduction of plasmonic nanostructure (red line). We attribute it to different SPPs resonance of the metal/dielectric interface. To quantify the collection efficiency in our simulation, we adopt a 0.5-NA water immersion objective with a detection limit of ±22° around the optic axis. Let us emphasize that the collimated beam with half width at half maximum of ±5° can be reached on the condition of optimal momentum matching for emission wavelength of 670 nm (see Fig. 7 of the Supporting Information). However, as mentioned previously, a large field enhancement factor actually comes at the expense of broad directivity. Nevertheless, the half width at half maximum of ±10° is still sufficient for the 0.5-NA water immersion objective with a collection efficiency of 77.2 %, compared to 40.7 % for a single slit without gratings.

Considering the modification of quantum efficiency in the emission process, we further study how the slit–groove structure affects the decay rate of a single molecule in the slit. Simulation results are summarized in Fig. 4 for nanostructures with and without gratings. As is well-known, the quantum efficiency would be modified when an emitter is placed in the vicinity of metallic nanostructures, which can be expressed as [26]:

$$\eta(\omega) = \eta_0(\omega) / \left[\frac{1 - \eta_0(\omega)}{F(\omega)} + \frac{\eta_0(\omega)}{\eta_a(\omega)} \right] \tag{2}$$

Here, $\eta_0(\omega)$ is the quantum efficiency in free space. Generally, we have the Purcell factor $F = \Gamma_{\mathrm{rad}} / \Gamma^0_{\mathrm{rad}} =$

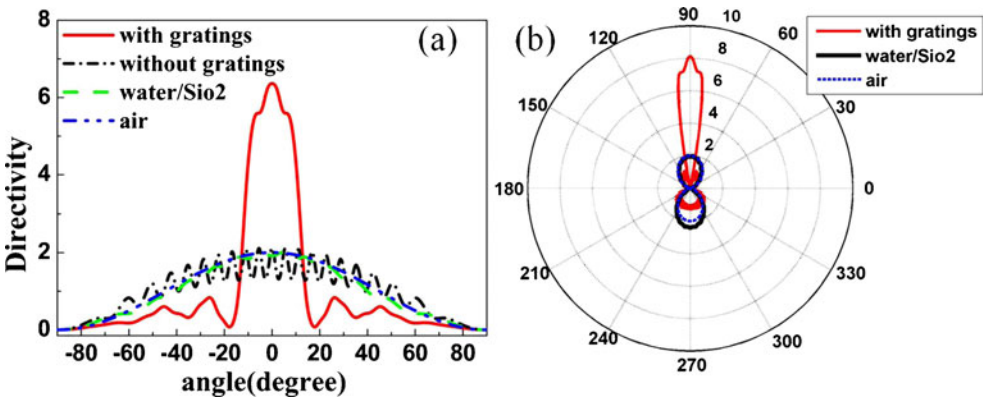

Fig. 3 **a** Calculated far-field directivities of a single dipole source (λ=670 nm) located inside the center of slit cavity (as well as the free space) radiated to the upper half space. **b** Normalized angular radiation pattern in the *x*–*z* plane of a dipole emission from a slit–groove structure (*red solid line*), compared to a dipole emission from the interface of water/SiO_2 (*black line*) and emission from air (*blue dashed line*)

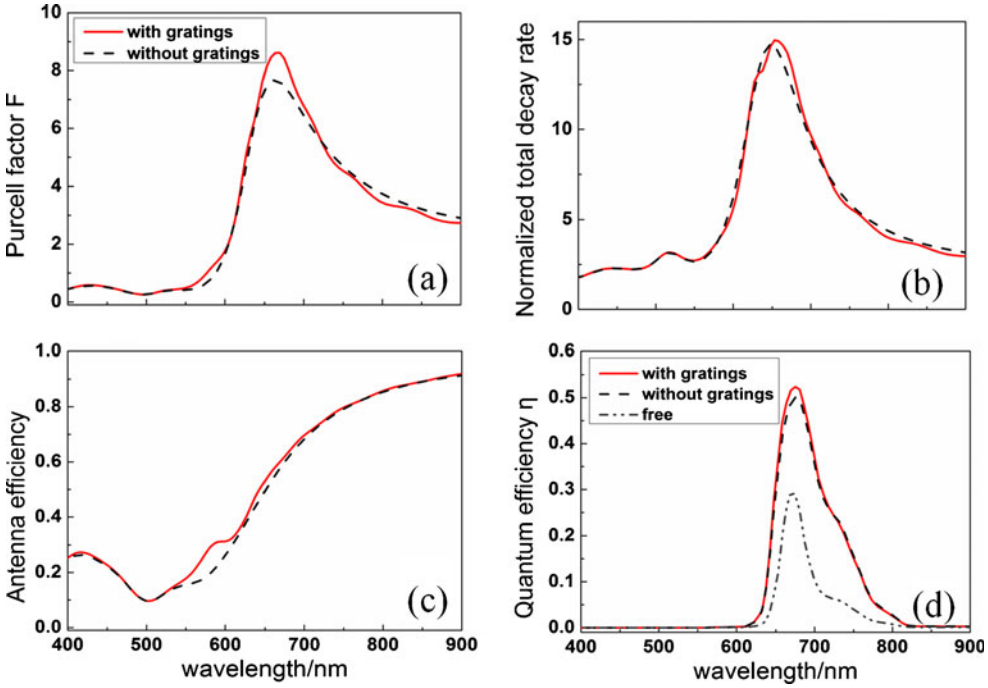

Fig. 4 **a** Purcell factor *F*, **b** normalized total decay rate, **c** antenna efficiency η_a, and **d** quantum efficiency η as a function of wavelength for the slit nanostructures with gratings (*solid line*) and without gratings (*dashed line*), respectively. The *gray dash–dot–dot line* in **d** represents the normalized spectrum of Cy5 dye in free solution

P_{rad}/P^0_{rad} (Fig. 4a) and the antenna efficiency $\eta_a = \Gamma_{rad}/\Gamma_{tot} = P_{rad}/P_{tot}$ (Fig. 4c), where the radiative decay rate Γ_{rad} (P_{rad}) or $\Gamma^0_{rad}(P^0_{rad})$ represents the energy radiated to the far field with or without metallic antennas. Additionally, the total decay rate $\Gamma_{tot}(P_{tot})$ represents all the energy emitted by a dipole, which is inversely proportional to the lifetime of a single molecule. For antenna structures without or with gratings, they behave similar to each other, as shown in Fig. 4. This indicates that the decay rates in the emission process are indeed modified by the slit cavity mainly and that is to say the Purcell enhancement primarily depends on the mode volume of the plasmonic slit cavity. It can be concluded that the grooves only affect the angular distributions strongly, but contribute little to the total radiated power (Fig. 4b). The results evidence previous reports [17, 18, 21] that the slit cavity determines the total decay rate or lifetime of a fluorescence molecule and primarily influences the quantum efficiency enhancement (Fig. 4d). A reference normalized spectrum of Cy5 dye in free solution is also presented for comparison and the intrinsic quantum efficiency $\eta_0(\omega)$ of Cy5 dye at λ~ 670 nm is set around 0.3 assumedly. We observe considerable quantum efficiency enhancements as well as small changes of spectrum shape in the presence of metallic antennas as shown in Fig. 4. Our results again are in good agreement with previous experimental studies [14, 17, 21].

Hereto, the excitation and emission gains discussed previously are summarized in Table 1 according to Eq. 1. Note that the dipole is placed in the center of the slit and we focus on the emission wavelength at 670 nm with intrinsic quantum efficiency $\eta_0 \sim 0.3$. For the slit–groove structure, we observe a significantly greater fluorescence enhancement factor of about 79.3 (relative to the free space). As we can see, the local excitation field enhancement factor plays a crucial role in the fluorescence enhancement. Additionally, the collection efficiency, taking advantage of the beaming effect, is twice as much as the single slit structure without gratings, while the quantum efficiency enhancements are almost unchanged for slits with or without the gratings. Furthermore, we plot the fluorescence enhancement as a function of initial quantum efficiency η_0 in solution, as demonstrated in Fig. 5. In the case of structure with gratings, the fluorescence enhancement factor depends strongly on the initial quantum efficiency and increases greatly with the decrease of η_0. For instance, the fluorescence enhancement factor increases from 79.3 to 154.4, while the initial quantum efficiency decreases from 0.3 to 0.13. The values appear quite similar to the performance of a bull' eyes structure reported in [17]. To make clear this phenomenon, we observe a saturation effect of the modified quantum efficiency at 670 nm when increasing the initial quantum efficiency η_0 (inset in Fig. 5), which seems to be a reasonable explanation. As the fluorescence enhancement is

Table 1 Contributions of excitation and emission gains to the total fluorescent enhancement

	I/I_0	k/k_0	η/η_0 (η_0~0.3)	S_f/S_{f0}
Without gratings	3.2	0.87	1.68	4.7
With gratings	27.5	1.65	1.75	79.3

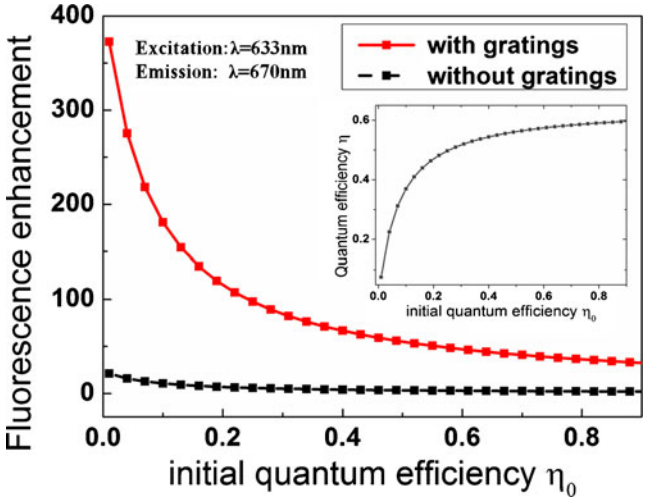

Fig. 5 Fluorescence enhancement S_f/S_{f0} as a function of the initial quantum efficiency η_0. η_0 is the quantum efficiency in solution without plasmonic antennas at 670 nm. *Inset* evolution of modified quantum efficiency η ($\lambda \sim 670$ nm) versus the initial quantum efficiency η_0

proportional to the quantum efficiency enhancement, the higher initial quantum efficiency usually results in the lower fluorescence enhancement.

In practice, it is not trivial to perform single-molecule detection in a subwavelength slit. The molecules with dilute concentration could be in solution diffusing freely in and out of the slit or fixed in a matrix on the surface with random orientations. For this reason, we select five representative dipole positions (A, B, C, D, and E) to further study the coupling of a single molecule with this slit–groove structure. Results are summarized in Fig. 6, showing that the fluorescence enhancement relies strongly on the dipole position. Figure 6a displays that the fluorescence enhancements of a dipole located in the central section of the slit (A, E) are the strongest, the outside edge (D) comes second, while the fluorescence enhancement of position C is slightly larger than position B. We point out that the coupling effects are largely determined by the field distribution (inset). To confirm this notion, we observe the far-field angular emission patterns (Fig. 6b) and quantum efficiencies (Fig. 6c) with different dipole positions. We find that dipole positions make very little difference to the emission directivities, but matter a lot to the power densities (inset of Fig. 6b). Except for the central section of the slit, the quantum efficiencies of the dipoles located in other places do not get obviously improved in comparison to the reference spectrum of Cy5 dye in free solution because of weak coupling to the antenna.

Conclusions

We theoretically explore the interaction of a single molecule with a slit–groove antenna in 2D FDTD simulations. The optimized structure for large fluorescence enhancement factor and narrow directivity is obtained by employing far-field radiation patterns calculated by NTFF transformation. We systematically quantify the excitation and emission gains in the total fluorescent enhancement. Simulation results confirm that the metal gratings strongly affect the local field enhancement and far-field angular distribution, yet affect

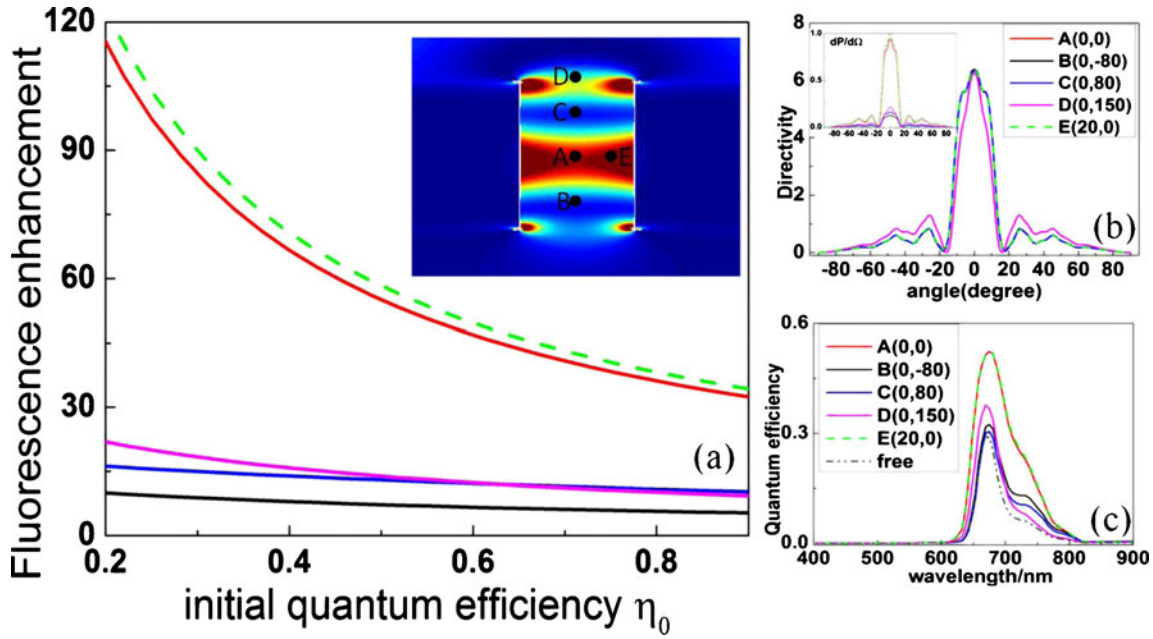

Fig. 6 Position dependence of fluorescence characteristics for a dipole source placed in an optimized slit–groove antenna: **a** total fluorescence enhancement S_f/S_{f0}, **b** far-field directivities, and **c** quantum efficiency

little on the total radiative rates. In other words, the lifetime of a single molecule is primarily determined by the slit cavity. We would like to stress here that the excitation and emission processes are strongly interlinked, which limits the flexibility to control the fluorescence emission to some extent. Although much effort is still needed to further optimize the antenna structure in three dimensions, our results give an instructive insight into the plasmonic-enhanced fluorescence based on the slit–groove structure.

Acknowledgments This work was supported by the National Basic Research Program of China (grant nos. 2013CB328703 and 2009CB930504) and the National Natural Science Foundation of China (grant nos. 61008026, 11121091, and 90921008).

References

1. Ahmed A, Gordon R (2012) Single molecule directivity enhanced Raman scattering using nanoantennas. Nano Lett 12:2625–2630
2. Ahmed A, Gordon R (2011) Directivity enhanced Raman spectroscopy using nanoantennas. Nano Lett 11:1800–1803
3. Lu G, Li W, Zhang T, Yue S, Liu J, Hou L, Li Z, Gong Q (2012) Plasmonic-enhanced molecular fluorescence within isolated bowtie nano-apertures. ACS Nano 6:1438–1448
4. Yang Z, Zhang Z, Hao Z, Wang Q (2011) Fano resonances in active plasmonic resonators consisting of a nanorod dimer and a nano-emitter. Appl Phys Lett 99:081107
5. Chen X, Agio M, Sandoghdar V (2012) Metallodielectric hybrid antennas for ultrastrong enhancement of spontaneous emission. Phys Rev Lett 108:233001
6. Lakowicz JR, Fu Y (2009) Modification of single molecule fluorescence near metallic nanostructures. Laser & Photonics Reviews 3:221–232
7. Fang Z, Lin C, Ma R, Huang S, Zhu X (2009) Planar plasmonic focusing and optical transport using CdS nanoribbon. ACS Nano 4:75–82
8. Fang Z, Peng Q, Song W, Hao F, Wang J, Nordlander P, Zhu X (2010) Plasmonic focusing in symmetry broken nanocorrals. Nano Lett 11:893
9. Lezec HJ, Degiron A, Devaux E, Linke RA, Martin-Moreno L, Garcia-Vidal FJ, Ebbesen TW (2002) Beaming light from a subwavelength aperture. Science 297:820–822
10. Levene MJ, Korlach J, Turner SW, Foquet M, Craighead HG, Webb WW (2003) Zero-mode waveguides for single-molecule analysis at high concentrations. Science 299:682–686
11. Yu N, Fan J, Wang QJ, Pflugl C, Diehl L, Edamura T, Yamanishi M, Kan H, Capasso F (2008) Small-divergence semiconductor lasers by plasmonic collimation. Nat Photon 2:564–570
12. Chee LT, Volodymyr VL, Kamal A, Yong TL (2010) Absorption enhancement of 980 nm MSM photodetector with a plasmonic grating structure. Opt Commun 283:1763–1767
13. Ishi T, Fujikata J, Ohashi K (2005) Si nano-photodiode with a surface plasmon antenna. Jpn J Appl Phys 44:L364–L366
14. García-Vidal FJ, Lezec HJ, Ebbesen TW, Martín-Moreno L (2003) Multiple paths to enhance optical transmission through a single subwavelength slit. Phys Rev Lett 90:213901
15. Martín-Moreno L, García-Vidal FJ, Lezec HJ, Degiron A, Ebbesen TW (2003) Theory of highly directional emission from a single subwavelength aperture surrounded by surface corrugations. Phys Rev Lett 90:167401
16. Wang C, Du C, Luo X (2006) Refining the model of light diffraction from a subwavelength slit surrounded by grooves on a metallic film. Phys Rev B 74:245403
17. Aouani H, Mahboub O, Bonod N, Devaux E, Popov E, Rigneault H, Ebbesen TW, Wenger J (2011) Bright unidirectional fluorescence emission of molecules in a nanoaperture with plasmonic corrugations. Nano Lett 11:637–644
18. Aouani H, Mahboub O, Devaux E, Rigneault H, Ebbesen TW, Wenger J (2011) Large molecular fluorescence enhancement by a nanoaperture with plasmonic corrugations. Opt Express 19:13056–13062
19. Fradin C, Abu-Arish A, Granek R, Elbaum M (2003) Fluorescence correlation spectroscopy close to a fluctuating membrane. Biophys J 84:2005–2020
20. Thio T, Pellerin KM, Linke RA, Lezec HJ, Ebbesen TW (2001) Enhanced light transmission through a single subwavelength aperture. Opt Lett 26:1972–1974
21. Jun YC, Huang KCY, Brongersma ML (2011) Plasmonic beaming and active control over fluorescent emission. Nat Commun 2:283
22. Zheng G, Cui X, Yang C (2010) Surface-wave-enabled darkfield aperture for background suppression during weak signal detection. Proc Natl Acad Sci 107:9043–9048
23. Aouani H, Mahboub O, Devaux E, Rigneault H, Ebbesen TW, Wenger J (2011) Plasmonic antennas for directional sorting of fluorescence emission. Nano Lett 11:2400–2406
24. Gérard D, Wenger J, Bonod N, Popov E, Rigneault H, Mahdavi F, Blair S, Dintinger J, Ebbesen TW (2008) Nanoaperture-enhanced fluorescence: towards higher detection rates with plasmonic metals. Phys Rev B 77:45413
25. Johnson PB, Christy RW (1972) Optical constants of the noble metals. Phys Rev B 6:4370–4379
26. Lu G, Zhang T, Li W, Hou L, Liu J, Gong Q (2011) Single-molecule spontaneous emission in the vicinity of an individual gold nanorod. J Phys Chem C 115:15822–15828
27. Huang KCY, Jun YC, Seo M, Brongersma ML (2011) Power flow from a dipole emitter near an optical antenna. Opt Express 19:19084–19092
28. Mahboub O, Palacios SC, Genet C, Garcia-Vidal FJ, Rodrigo SG, Martin-Moreno L, Ebbesen TW (2010) Optimization of bull's eye structures for transmission enhancement. Opt Express 18:11292–11299
29. Taflove A, Hagness SC (2005) Computational electrodynamics: the finite-difference time-domain method, 3rd edn. Artech House, Norwood
30. Kim S, Kim S, Lee Y (2006) Vertical beaming of wavelength-scale photonic crystal resonators. Phys Rev B 73:235117
31. Kühn S, Håkanson U, Rogobete L, Sandoghdar V (2006) Enhancement of single-molecule fluorescence using a gold nanoparticle as an optical nanoantenna. Phys Rev Lett 97:17402
32. Bonod N, Popov E, Gérard D, Wenger J, Rigneault H (2008) Field enhancement in a circular aperture surrounded by a single channel groove. Opt Express 16:2276–2287
33. Lee KG, Chen XW, Eghlidi H, Kukura P, Lettow R, Renn A, Sandoghdar V, G tzinger S (2011) A planar dielectric antenna for directional single-photon emission and near-unity collection efficiency. Nat Photon 5:166–169